Am J Cancer Res 2017;7(7):1463-1475
www.ajcr.us /ISSN:2156-6976/ajcr0057318

Original Article

Long non-coding RNA DGCR5 is involved in the regulation of proliferation, migration and invasion of lung cancer by targeting miR-1180

En-Guo Chen, Ji-Song Zhang, Shan Xu, Xiao-Jing Zhu, Hui-Hui Hu

Department of Pulmonary Medicine, Sir Run Run Shaw Hospital of Zhejiang University, Hangzhou 310016, Zhejiang Province, China

Received May 12, 2017; Accepted May 23, 2017; Epub July 1, 2017; Published July 15, 2017

Abstract: Accumulating studies have demonstrated that non-coding RNAs (ncRNAs), including small non-coding RNAs (small ncRNAs) and long non-coding RNAs (lncRNAs), are involved in tumor growth in lung cancer (LC). However, the specific role of DGCR5 in LC progression is not yet clear. In the present study, we found that DGCR5 was downregulated and miR-1180 was upregulated in the sera and tissues of LC patients and was correlated with poor prognosis. We also found that DGCR5 suppressed proliferation, migration and invasion of LC cell lines H520 and H1299. In addition, a luciferase reporter gene assay was used to investigate the regulatory relationship between DGCR5 and miR-1180. Furthermore, we suggested that DGCR5 inhibited the expression of AKT, GSK-3β, and β-catenin by targeting miR-1180. Based on these findings, DGCR5 might serve as a potential target for the development of effective anti-neoplastic therapies in lung cancer.

Keywords: Long non-coding RNA DGCR5, miR-1180, lung cancer, migration and invasion

Introduction

Lung cancer, including non-small cell LC (NSCLC) and small cell LC (SCLC), is a principle cause of cancer-associated mortality in both developed and developing countries [1, 2]. In 2016, LC accounted for 224390 new cases and 158080 deaths in the United States, and most of the LC patients (approximately 80%) had NSCLC [3, 4]. Despite the substantial progress in novel treatments in the last few decades, the five-year relative survival of LC is only 10-15% [5, 6]. The high incidence and poor prognosis of LC are mainly due to the lack of effective measures for diagnosis and treatment, and patients are often diagnosed at advanced stages [7-9]. The current therapies for LC patients mainly include chemotherapy and radiotherapy, with very limited therapeutic efficacy and several unexpected side effects [8, 10-12]. Therefore, it is urgent to determine the underlying molecular mechanisms of LC.

Non-coding RNAs (ncRNAs), characterized by the lack of coding potential, consist of two subgroups according to their relative size-small non-coding RNAs (sncRNAs, shorter than 200 nucleotides) and long non-coding RNAs (lncRNAs, longer than 200 nucleotides) [13-16]. The subgroup of small ncRNAs include the well-documented microRNAs (miRNAs), which are only 22 nucleotides in length and have been reported as being the primary regulators of expression of numerous genes by controlling the translation of mRNA into proteins [17, 18]. Previous studies have indicated that miRNAs are involved in regulating many biological processes in various cancers [19, 20]. In addition to miRNAs, increasing evidence has also indicated that lncRNAs are involved in the pathogenesis of LC. Li et al. have reported that lncRNA prostate cancer-associated transcript 6 (PCAT6) is upregulated in LC, and knockdown of lncRNA PCAT6 promotes proliferation and invasion of tumor cells [21]. lncRNA urothelial carcinoma-associated 1 (UCA1) has been found to be upregulated in NSCLC tissues, and overexpression of lncRNA UCA1 has been shown to inhibit tumor cell growth by increasing the miR-193a-3p target gene ERBB4 [22]. Recently, a novel lncRNA DiGeorge syndrome critical region gene 5 (DGCR5) was found to be down-

regulated in hepatocellular carcinoma (HCC), and low expression of DGCR5 was closely associated with poor five-year survival rate [23]. However, few studies have reported the role of DGCR5 in LC.

miRNAs, a class of non-coding RNA approximately 20 nucleotides long, are involved in post-transcriptional regulation, which affects biological processes by targeting the 3'-UTR of target genes [24-26]. Studies have indicated that miRNAs play important roles in the development of human cancers [24, 27]. In this study, we will explore the functional relevance of miR-1180 in LC.

In the present study, we explored the expression levels of DGCR5 and miR-1180 in the sera and tissues of LC patients, their correlation with poor prognosis, the regulatory relationship between DGCR5 and miR-1180, and the influence of DGCR5 on the proliferation, migration and invasion of LC cells through miR-1180. In addition, we demonstrated the effect of DGCR5 on the regulation of expression of AKT, GSK-3β, and β-catenin through miR-1180. Therefore, this study was conducted to determine whether DGCR5 is associated with LC and to identify the underlying molecular mechanisms.

Materials and methods

Clinical specimens

This study was approved by the ethical committee of Sir Run Run Shaw Hospital. The tissues and sera used in this study were collected from LC patients in Sir Run Run Shaw Hospital from June 2012 to June 2014. None of the patients had undergone radiotherapy or chemotherapy before surgical resection. Adjacent normal tissues were collected from a site at least 5 cm away from the tumor, and all samples were examined histologically. Informed consent was obtained from every patient. All tissue samples were store at -80°C. In addition, 5 ml of blood was collected from 40 patients with LC as well as from healthy controls; the serum was separated by centrifugation after 2 hr, and the supernatant was frozen at -80°C until analysis.

Cells culture

Human lung epithelial cells (BEAS-2B), LC cell lines (H520, H157, SKMES1, H460, A549, and H1299), and human embryonic kidney 293T (HEK293T) cells were purchased from American Type Culture Collection (ATCC). BEAS-2B, H520, H157, H1299 and H460 cells were cultured in RPMI 1640 medium (Invitrogen); A549 cells were cultured in Ham's F12 media (Cellgro); SKMES-1 cells were cultured in EMEM media (Fisher Scientific). HEK293T cells were cultured in Dulbecco's Modified Eagle's Medium (DMEM; Invitrogen, Carlsbad, CA, USA). All media were supplemented with 10% fetal bovine serum (FBS; Invitrogen, Carlsbad, CA, USA) and penicillin/streptavidin (final concentration 50 μg/ml; Sigma-Aldrich, St. Louis, MO, USA). All cells were cultured at 37°C in a humidified incubator constantly supplied with 5% CO_2.

Lentiviral vector construction, production and transfection

Full-length cDNA for human DGCR5 was amplified by PCR from mRNA of H520 cells and inserted into a lentiviral vector. A lentiviral vector expressing Green Fluorescent Protein (GFP) was used as the control. shDGCR5 sequences to target human DGCR5 were designed, generated and cloned into human U6 promoter-containing pBluescript SK (+) plasmid (pU6). U6 was then cloned into a lentiviral vector. shLUC was used as the negative control (NC). The constructed vectors and three packaging vectors (pMDLg/pRRE, pRSV-REV and pCMV-VSVG) were co-transfected into HEK293T cells to produce viral particles for lentiviral transduction. H1299 and H520 cells (5×10^4 cells/well) were seeded in 24-well plates and then transduced with the lentiviruses using 8 μg/ml polybrene (Sigma-Aldrich, St. Louis, MO, USA).

miRNA transfection

miR-1180 mimics, miR-1180 inhibitors, mimics NC, inhibitors NC were obtained from Thermo Fisher Scientific, Inc. H1299 cells transduced with Lenti-DGCR5 (2×10^5 cells/well) were cultured in 6-well plates and then transfected with 200 μl mature miR-1180 mimics or mimics NC (GenePharma Co., Ltd., Shanghai, China) for 72 hrs; H520 cells transduced with shDGCR5 (2×10^5 cells/well) were cultured in 6-well plates and then transfected with 200 μl mature miR-1180 inhibitors or inhibitors NC (GenePharma Co., Ltd., Shanghai, China) for 72 hrs. All transfections were completed using Lipofectamine™ 3000 (Invitrogen, Carlsbad, CA, USA) according

Table 1. Primer sequences for qRT-PCR analysis

Gene	Primer sequences
GAPDH	Forward: 5'-TATGATGATATCAAGAGGGTAGT-3'
	Reverse: 5'-TGTATCCAAACTCATTGTCATAC-3'
DGCR5	Forward: 5'-CCAAGCCTGTCTGTGTGTTC-3'
	Reverse: 5'-GGGAGACACAGACCACAAGA-3'
miR-1180	Forward: 5'-CAGAAACAGCCATCCCAGAG-3'
	Reverse: 5'-GCCTTCAGCAGGATGTCAAT-3'
U6	Forward: 5'-CTCGCTTCGGCAGCACA-3'
	Reverse: 5'-AACGCTTCACGAATTTGCGT-3'
AKT	Forward: 5'-ACGTAGCCATTGTGAAGGAGG-3'
	Reverse: 5'-TGCCATCATTCTTGAGGAGGAA-3'
β-catenin	Forward: 5'-GACTTCACCTGACAGATCCAAG-3'
	Reverse: 5'-AGCTGAACAAGAGTCCCAAG-3'
GSK3β	Forward: 5'-CTGGGACGACATGGAGAAAA-3'
	Reverse: 5'-AAGGAAGGCTGGAAGAGTGC-3'

to the manufacturer's protocols. The transfection efficiency was assessed by qRT-PCR.

qRT-PCR

Total RNA was extracted using TRIzol (Invitrogen) according to the manufacturer's instructions. Then, cDNA synthesis was performed using Revert Aid First Strand cDNA Synthesis Kit (Thermo Fisher Scientific Inc., Rockford, IL, USA). The mRNA expression level was evaluated by qRT-PCR with SYBR Green PCR Master Mix (Applied Biosystems, Warrington, U.K.) and an ABI 7500 Real-time PCR system (Applied Biosystems). The results were calculated using the $2^{-\Delta\Delta Ct}$ method. The primers specific for target genes and GAPDH (internal loading control) were designed and are shown in **Table 1**.

Western blot analysis

Cells were lysed on ice in radioimmunoprecipitation (RIPA, Pierce Biotechnology, cat. no. 8990) buffer containing protease inhibitor cocktail (Thermo Fisher Scientific, Inc.). The BCA protein assay kit (Qcbio Science Technologies Co., Ltd., Shanghai, China) was used to the detection of protein concentration. Total protein (30 μg) was separated by 10% SDS-PAGE and transferred to PVDF membranes (Bio-Rad Laboratory, USA). The membranes were blocked with 5% skim milk (BD Biosciences) and incubated with primary antibodies overnight at 4°C. The next day, the membranes were incubated with horseradish peroxidase (HRP)-conjugated secondary antibodies (Sigma-Aldrich cat. #A6154) for 2 hrs at room temperature. Protein levels were measured using an ECL system (Amersham Pharmacia Biotech). The results were analyzed with Image Lab Software version 4.1 (Bio Rad). The primary antibodies were anti-β-catenin antibody (dilution 1:1000; Abcam, #2982), anti-AKT antibody (dilution 1:1000, Cell Signaling, Boston, MA, USA; 4685), anti-p-AKT antibody (dilution 1:1000, Cat. No. 4058s, Cell Signaling Technology Inc., Danvers, MA, USA), anti-GSK3β antibody (dilution 1:1000, Abcam, Cat. No. ab757-45) and anti-GAPDH antibody (dilution 1:1000; Santa Cruz Biotechnology, Santa Cruz, CA, USA, Cat. No. sc-365062).

Luciferase reporter assay

H1299 cells were cultured in 24-well plate at a density of 5×10^4 cells/well and cotransfected with miR-1180 mimic, mimic negative control, WT or Mut 3'-UTR of DGCR5, and Renilla plasmid (RL-SV40, Promega). Cells were collected and lysed in Passive Lysis Buffer (Promega, WI, USA) 48 hrs after transfection. The relative fluorescence value was detected using a Dual-Luciferase® Reporter Assay Kit (Promega). The Dual-Luciferase Reporter Assay System (Promega, Wisconsin, WI, USA) was used to analyze the data.

Cell proliferation assay

The transfected H1299 and H520 cells were seeded in 96-well plates with 100 μL medium (10% FBS) at a density of 2×10^3 cells/well and cultured at 37°C with 5% CO_2. Twenty microliters of MTT solution (5 mg/ml) was added into each well at a given point in time. Then, the cells were incubated for 4 hrs at 37°C. Two hundred microliters of dimethyl sulfoxide (DMSO) was added into each well to dissolve the formazan product for 10 mins at room temperature. The absorbance at 490 nm was measured using an Elx800 Reader (Bio-Tek Instruments Inc., Winooski, VT, USA).

Colony formation assay

Transfected H1299 and H520 cells (500 cells/well) were seeded in 6-well plates. The plates were incubated for 14 days at 37°C, and the medium was replaced every 3 days. Then, the cells were washed with PBS, fixed with 4% paraformaldehyde and then stained with 0.5% crystal violet. Images of colonies were obtained

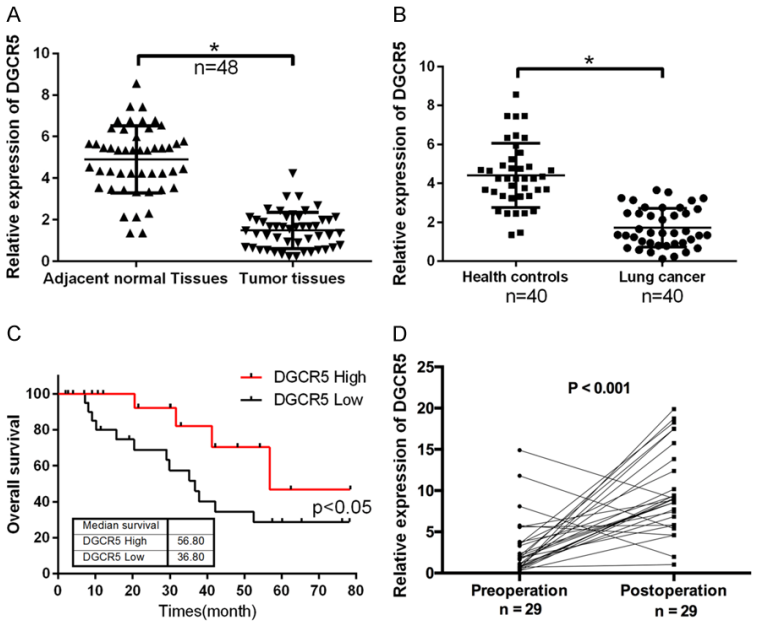

Figure 1. DGCR5 was downregulated in the sera and tissues of LC patients and was associated with poor prognosis. A. DGCR5 expression was detected by qRT-PCR in LC samples and corresponding normal lung tissues (n = 48, **P* < 0.05). B. qRT-PCR was used to analyze the expression level of DGCR5 in the sera of LC patients (n = 40) and healthy controls (n = 40, **P* < 0.05). C. Kaplan-Meier survival analysis was used to assess the effect of DGCR5 on LC prognosis (*P* < 0.05). D. qRT-PCR was performed to measure the changes in the expression of DGCR5 between pre-operation and post-operation serum samples from LC patients (n = 29, *P* < 0.01).

using a microscope. The number of the colonies was counted.

Cell migration and invasion assays

The migratory and invasive abilities were detected using Transwell cell culture chambers (Corning Costar Corp, Cambridge, MA, USA) with or without 10 μl Matrigel (diluted 1:3; BD Biosciences, San Jose, CA, USA). Transfected H1299 and H520 cells (5 × 10^5/200 μl) were added to upper chambers, and complete medium was added to the lower chambers. After incubation at 37°C for 24 hrs, migratory and invasive cells were fixed using 4% paraformaldehyde and stained with 0.1% crystal violet solution. Five randomly selected fields from each membrane were counted using a light microscope.

Statistical analysis

The data are presented as the mean values ± standard deviation (SD), and differences were considered statistically significant at *P* < 0.05. SPSS 21.0 (SPSS, Inc., Chicago, IL, USA) and GraphPad (GraphPad Prism Software, La Jolla, CA, USA) were used to perform the analyses.

Results

DGCR5 was downregulated in the sera and tissues of LC patients and was associated with poor prognosis

To estimate the expression status and possible prognostic impact of DGCR5 in LC, the expression level of DGCR5 was determined by qRT-PCR in LC samples and corresponding normal lung tissues from 48 patients. The results indicated that DGCR5 was expressed at a lower level in LC tissues than in the adjacent normal tissues (*P* < 0.05, **Figure 1A**). DGCR5 expression was also analyzed in the sera of LC patients (n = 40) and healthy controls (n = 40), and the results also revealed that DGCR5 was downregulated in the sera of LC patients compared with the sera of healthy controls (*P* < 0.05, **Figure 1B**). The relationship between DGCR5 expression and different clinicopathologic features (age, gender, lymph node metastasis, distant metastasis, and TNM stage) was analyzed (**Table 2**). In addition, the LC patients were divided into high expression group and low expression group according to the expression level of DGCR5 (median split), and Kaplan-Meier analysis was used to assess the effect of DGCR5 on LC prognosis. We found that higher expression of DGCR5 was associated with longer survival in LC patients (*P* < 0.05, **Figure 1C**). The change in expression of DGCR5 was further analyzed by qRT-PCR in pre-operation and post-operation sera of LC patients (n = 29). The data showed that DGCR5 expression was increased in the post-operation sera compared with that in the pre-operation sera (*P* < 0.001, **Figure 1D**). These results demonstrated that DGCR5 expression was downregulated in LC tissues and correlated with poor outcome of LC patients.

Table 2. The relationship between DGCR5 expression level (ΔCt) and clinicopathological features of LC patients

Characteristics	No. of patients (%)	DGCR5	
		Mean ± SD	*P* value
Total no. of patients	48		
Age (year)			
> 60	35 (72.9)	11.28 ± 1.04	0.615
≤ 60	13 (27.1)	11.46 ± 1.24	
Gender			
Male	38 (79.2)	11.05 ± 1.49	0.444
Female	10 (20.8)	11.48 ± 1.85	
Lymphatic metastasis			
N0	29 (60.4)	11.14 ± 1.24	0.023*
N1-N2	19 (39.6)	11.99 ± 1.19	
Distal metastasis			
M0	39 (81.3)	11.21 ± 1.28	0.189
M1	9 (18.7)	11.85 ± 1.38	
TNM stage			
0 & I & II	40 (83.3)	11.25 ± 1.78	0.287
III & IV	8 (16.7)	12.04 ± 2.34	

*Indicates $P < 0.05$.

DGCR5 inhibited proliferation, migration and invasion of LC cells

To investigate the roles of DGCR5 on proliferation, migration and invasion of LC cells, we first analyzed the expression level of DGCR5 using qRT-PCR in human lung epithelial cells (BEAS-2B) and LC cell lines (H520, H157, SKMES1, H460, A549, and H1299) and found that it was dramatically decreased in the LC cell lines compared with that in BEAS-2B cells. Among the LC cells, the expression level of DGCR5 was lowest in H1299 cells and highest in H520 cells (*$P < 0.05$ and **$P < 0.01$, **Figure 2A**). Therefore, we selected the H1299 and H520 cells as target cells. In our study, H1299 cells were transduced with GFP-encoding lentivirus (Lenti-GFP, control) and DGCR5 lentivirus (Lenti-DGCR5). H520 cells were transduced with shLuc (lentiviral vector-mediated shRNA against Luc, control) and shDGCR5 (lentiviral vector-mediated shRNA against DGCR5). First, the expression level of DGCR5 was detected by qRT-PCR, and the results showed that DGCR5 was expression was markedly high in the H1299 cells transfected with Lenti-DGCR5 compared with the cells transfected with Lenti-GFP ($P < 0.001$); moreover, DGCR5 expression was significantly low in H520 cells transfected with shDGCR5 compared with those transfected with shLuc ($P < 0.001$, **Figure 2B**). Furthermore, MTT and colony formation assays were performed to measure the proliferative abilities of the transfected H520 and H1299 cells. As shown in **Figure 2C** and **2D**, DGCR5 significantly suppressed cell growth of H1299 and H520 cells. Silencing of DGCR5 significantly accelerated the proliferative abilities of H1299 and H520 cells ($P < 0.001$). Furthermore, the impacts of DGCR5 on cell migration and invasion were evaluated by Transwell assays *in vitro*. The results revealed that DGCR5 markedly inhibited migration and invasion of LC cells. Silencing of DGCR5 clearly promoted the migration and invasion of LC cells ($P < 0.001$, **Figure 2E**). These data suggested that DGCR5 was involved in regulating the proliferation, migration and invasion of LC cells.

Screening for DGCR5-regulated miRNAs in LC

To investigate the relationships between DGCR5 and miRNAs, we predicted the miRNAs that may interact with DGCR5 using RegRNA (Supplementary Table 1). The cutoff for the mfe was set at -26, because the lower free energy represented a more stable interaction between the miRNA and lncRNA. In addition, we performed gene microarray analysis to screen for differentially expressed miRNAs associated with LC (data not shown). Thus, 5 miRNAs including let-7b, miR-1180, miR-324-5p, miR-663, and miR-762 were selected. Furthermore, qRT-PCR was performed to validate the expression levels of these miRNAs in H520 and H1299 cells. Our results revealed that miR-1180 was expressed at the lowest level in DGCR5-overexpressing H1299 cells and was expressed at the highest level in DGCR5-silenced H520 cells (**Figure 3A**, **3B**). Therefore, miR-1180 was selected for further study.

miR-1180 was upregulated in the sera and tissues of LC patients and was correlated with poor prognosis

To further evaluate the expression level of miR-1180 in LC, qRT-PCR was used. We found that miR-1180 expression was elevated in LC tissues compared with that in the paired non-tumor tissues (n = 48, ***$P < 0.001$, **Figure 4A**). miR-1180 was also upregulated in the sera of LC patients compared with those of healthy controls (n = 40, ***$P < 0.001$, **Figure 4B**). The

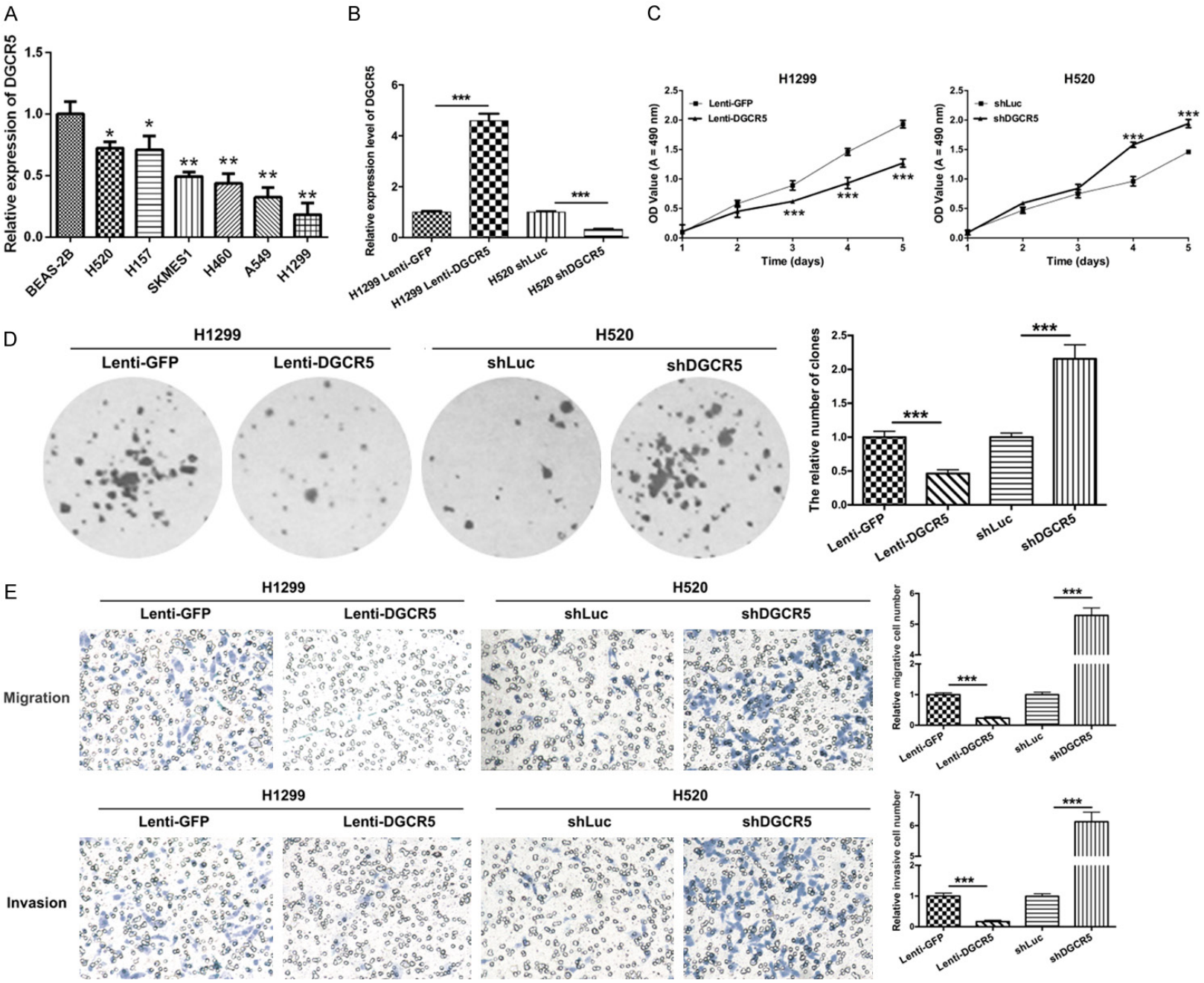
A
Relative expression of DGCR5
BEAS-2B
H520
H157
SKMES1
H460
A549
H1299
B
Relative expression level of DGCR5
H1299 Lenti-GFP
H1299 Lenti-DGCR5
H520 shLuc
H520 shDGCR5
C
H1299
Lenti-GFP
Lenti-DGCR5
OD Value (A = 490 nm)
Time (days)
H520
shLuc
shDGCR5
D
H1299
Lenti-GFP
Lenti-DGCR5
H520
shLuc
shDGCR5
The relative number of clones
E
Migration
Invasion
Relative migrative cell number
Relative invasive cell number

Figure 2. DGCR5 inhibited proliferation, migration and invasion of LC cells. A. The relative expression of DGCR5 was detected by qRT-PCR in human lung epithelial cells (BEAS-2B) and LC cell lines (H520, H157, SKMES1, H460, A549, and H1299, $*P < 0.05$, $**P < 0.01$). B. H1299 cells were transduced with GFP-expressing lentivirus (Lenti-GFP, control) and DGCR5 lentivirus (Lenti-DGCR5). H520 cells were transduced with shLuc (lentiviral vector-mediated shRNA against Luc, control) and shDGCR5 (lentiviral vector-mediated shRNA against DGCR5). Then, qRT-PCR was used to detect the expression level of DGCR5 ($***P < 0.001$). C. MTT assay was performed to detect the proliferative abilities of the transfected H520 and H1299 cells ($***P < 0.001$). D. The clonogenic capacities were measured by the colony formation assay in the transfected H520 and H1299 cells ($***P < 0.001$). E. Transwell assays were performed to analyze the migration and invasion abilities of H1299 cells transduced with Lenti-GFP or Lenti-DGCR5 and H520 cells transduced with shLuc or shDGCR5 (Magnification, × 200, $***P < 0.001$).

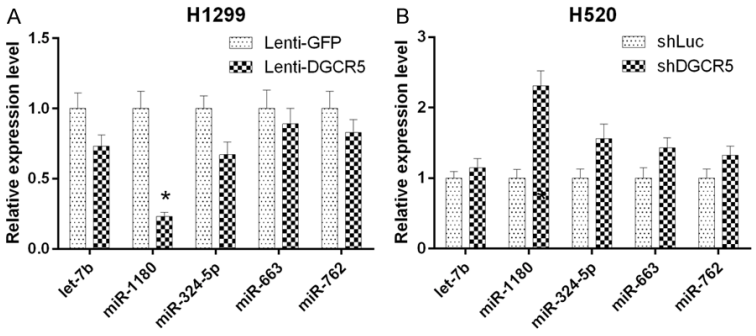

Figure 3. Screen for DGCR5-regulated miRNAs in LC cells. A. The expression of selected miRNAs let-7b, miR-1180, miR-342-5p, miR-663 and miR-764 was confirmed by qRT-PCR in DGCR5 overexpressing H1299 cells. B. The expression of selected miRNAs was confirmed by qRT-PCR in DGCR5-silenced H520 cells ($*P < 0.05$).

results of Kaplan-Meier survival analysis also showed that higher expression of miR-1180 was associated with shorter survival in LC patients ($P < 0.05$, **Figure 4C**). MiR-1180 expression was then analyzed by qRT-PCR in pre-operation and post-operation sera of LC patients (n = 29), and the results revealed that miR-1180 expression was lower in the post-operation sera compared with that in the pre-operation sera ($P < 0.001$, **Figure 4D**). We also found that miR-1180 was significantly related to TNM stage ($P = 0.025$) by clinicopathological analysis of LC tissues (**Table 3**). In addition, the relationship between DGCR5 and miR-1180 in LC tissues and sera was analyzed. The result indicated that there was a negative correlation between DGCR5 and miR-1180 expression in LC tissues ($R^2 = 0.11$, $P = 0.021$, **Figure 4E**) and sera ($R^2 = 0.138$, $P = 0.018$, **Figure 4F**). Therefore, we speculated that DGCR5 regulates miR-1180 expression in LC.

DGCR5 suppressed proliferation, migration and invasion of LC cells by targeting miR-1180

To determine whether DGCR5 interacts with miR-1180 to regulate transcription in LC cells, we hypothesized that DGCR5 directly regulates miR-1180 expression and cloned the wild-type or mutant DGCR5 into pGL3-basic luciferase reporter vector. Luciferase reporter gene assays demonstrated that DGCR5 weakened the luciferase activity ($***P < 0.001$, **Figure 5A**). In addition, we treated H1299 cells with Lenti-GFP, Lenti-DGCR5, Lenti-DGCR5 and mimics NC, or Lenti-DGCR5 and miR-1180 mimics and treated H520 cells with shLuc, shDGCR5, shDGCR5 and inhibitors NC, or shDGCR5 and miR-1180 inhibitors. The results from qRT-PCR showed that DGCR5 inhibited miR-1180 expression, and miR-1180 mimics promoted miR-1180 expression. Silencing of DGCR5 promoted miR-1180 expression, and miR-1180 inhibitors suppressed miR-1180 expression ($***P < 0.001$, **Figure 5B**). Subsequently, we performed MTT assay to detect the proliferative ability of LC cells and found that DGCR5 markedly inhibited proliferation of LC cells, and miR-1180 mimics promoted it via DGCR5 in H1299 cells ($***P < 0.001$, **Figure 5C**). Similarly, silencing of DGCR5 significantly increased the proliferation of LC cells, and miR-1180 inhibitors reduced the DGCR5-silencing-induced increase in proliferation ($***P < 0.001$, **Figure 5D**). Furthermore, we found that DGCR5 significantly decreased migration and invasion of H1299 cells, and miR-1180 mimics blocked this DGCR5-induced decrease ($***P < 0.001$, **Figure 5E**). Silencing of DGCR5 significantly promoted the migration and invasion of H520 cells, and miR-1180 inhibitors then inhibited this DGCR5-silencing-induced promotion ($***P < 0.001$, **Figure 5F**). Therefore, we suggested that DGCR5 suppre-

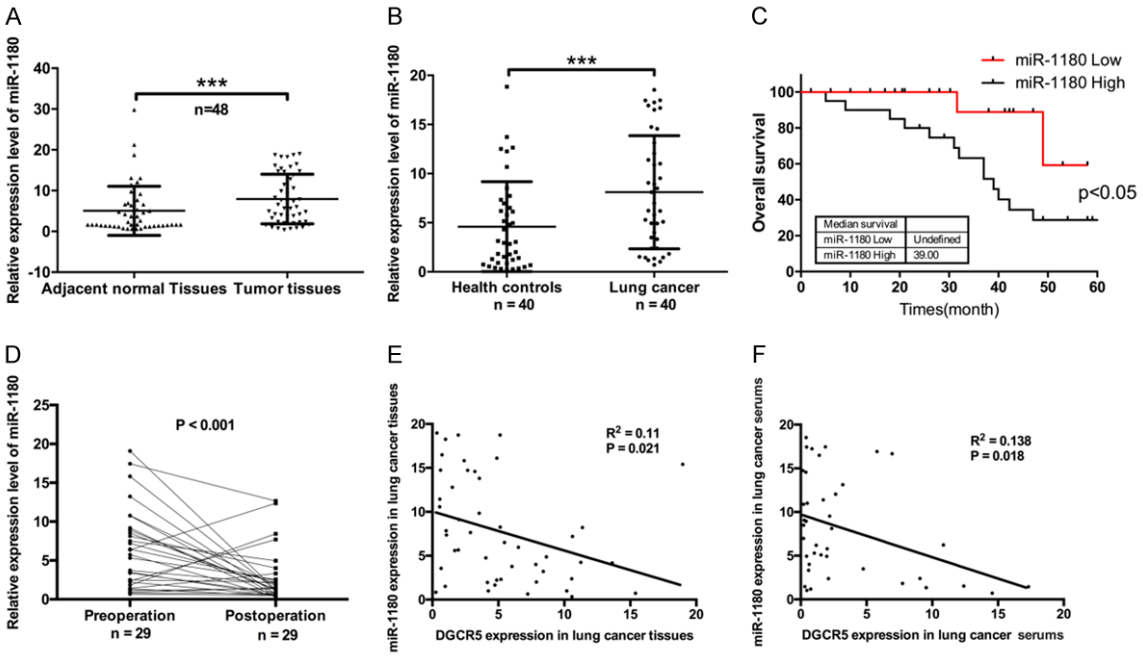

Figure 4. miR-1180 was upregulated in the sera and tissues of LC patients and was correlated with poor prognosis. A. Relative mRNA expression of miR-1180 was detected by qRT-PCR in LC tissues and paired non-tumor tissues (n = 48, ***P < 0.001). B. miR-1180 expression was analyzed by qRT-PCR in the sera of LC patients (n = 40) and healthy controls (n = 40, ***P < 0.001). C. Kaplan-Meier survival analysis was conducted according to miR-1180 expression level in LC patients. D. qRT-PCR was used to detect miR-1180 expression in the pre-operation and post-operation serum samples of LC patients (n = 29, P < 0.05). E. Analysis of correlation between DGCR5 and miR-1180 in LC tissues (n = 48, R^2 = 0.11, P < 0.05). F. Analysis of correlation between DGCR5 and miR-1180 in LC sera (n = 40, R^2 = 0.138, P < 0.05).

Table 3. The relationship between miR-1180 expression level (ΔCt) and clinicopathological features of LC patients

Characteristics	No. of patients (%)	miR-1180	
		Mean ± SD	*P* value
Total no. of patients	48		
Age (year)			
> 60	35 (72.9)	10.45 ± 1.35	0.329
≤ 60	13 (27.1)	10.86 ± 1.05	
Gender			
Male	38 (79.2)	10.43 ± 1.31	0.741
Female	10 (20.8)	10.58 ± 1.08	
Lymphatic metastasis			
N0	29 (60.4)	10.13 ± 1.37	0.418
N1-N2	19 (39.6)	10.43 ± 1.02	
Distal metastasis			
M0	39 (81.3)	11.32 ± 1.47	0.345
M1	9 (18.7)	10.82 ± 1.13	
TNM stage			
0 & I & II	40 (83.3)	11.52 ± 1.28	0.025*
III & IV	8 (16.7)	10.34 ± 1.49	

*Indicates P < 0.05.

ssed proliferation, migration and invasion of LC cells by targeting miR-1180.

DGCR5 decreased the expression levels of AKT, GSK-3β, and β-catenin through miR-1180

In addition, we further analyzed the impacts of DGCR5 on the expression levels of AKT, GSK-3β, and β-catenin through miR-1180. The expression levels of AKT, GSK-3β, and β-catenin were measured by qRT-PCR and Western blotting. The results showed that the expression levels of AKT, GSK-3β, and β-catenin were markedly downregulated in H1299 cells transfected with Lenti-DGCR5 compared with those in cell transfected with Lenti-GFP (***P < 0.001). The expression levels of AKT, GSK-3β, and β-catenin were also dramatically increased in H1299 cells transfected with Lenti-DGCR5 and miR-

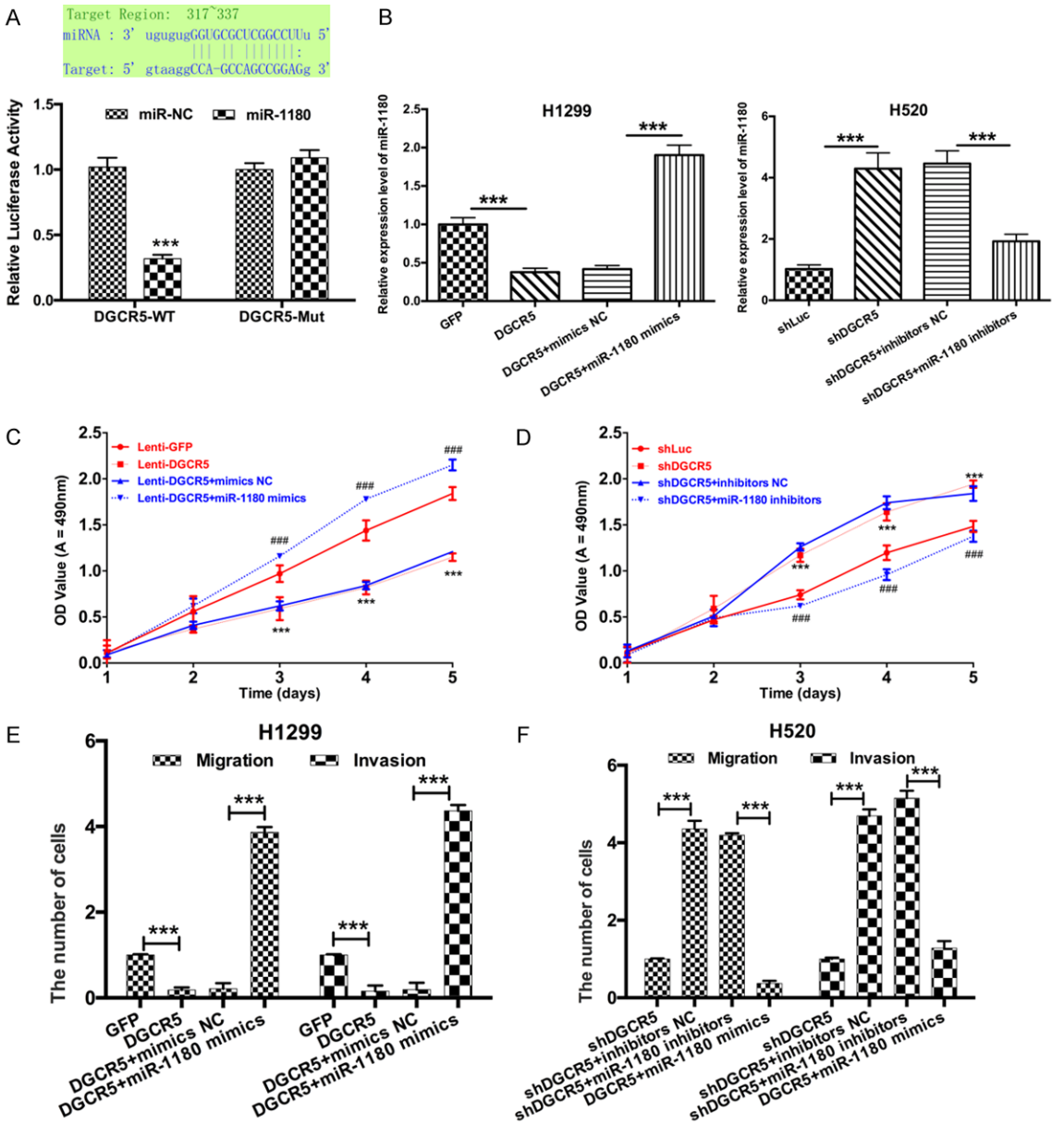

Figure 5. DGCR5 suppressed proliferation, migration and invasion of LC cells by targeting miR-1180. (A) The relative fluorescence was detected by the luciferase reporter gene assay in H1299 cells co-transfected with wild = type DGCR5 or mutant DGCR5 and miR-NC or miR-1180 (***$P < 0.001$). H1299 cells were transduced with Lenti-GFP, Lenti-DGCR5, Lenti-DGCR5 and mimics NC or Lenti-DGCR5 and miR-1180 mimics; H520 cells were transduced with shLuc, shDGCR5, shDGCR5 and inhibitors NC or shDGCR5 and miR-1180 inhibitors. miR-1180 expression was detected by qRT-PCR (B, ***$P < 0.001$). The proliferative abilities of H1299 and H520 cells were assessed by MTT assay (C and D, ***$P < 0.001$). The migration and invasion of H1299 and H520 cells were measured by Transwell assay (E and F, Magnification, × 200, ***$P < 0.001$).

1180 mimics compared with cells transfected with Lenti-DGCR5 and mimics NC (***$P < 0.001$, **Figure 6A** and **6C**). Similarly, silencing of DGCR5 markedly promoted the expression of AKT, GSK-3β, and β-catenin, and then miR-1180 inhibitors abrogated the DGCR5-silencing-induced promotion (***$P < 0.001$, **Figure 6B** and **6D**).

Discussion

lncRNAs, one of the most important classes of non-coding RNAs, are thought to be critical gene regulators via their binding to corresponding mRNAs [28]. An increasing number of studies have found that lncRNAs participate in the development and progression of some cancers

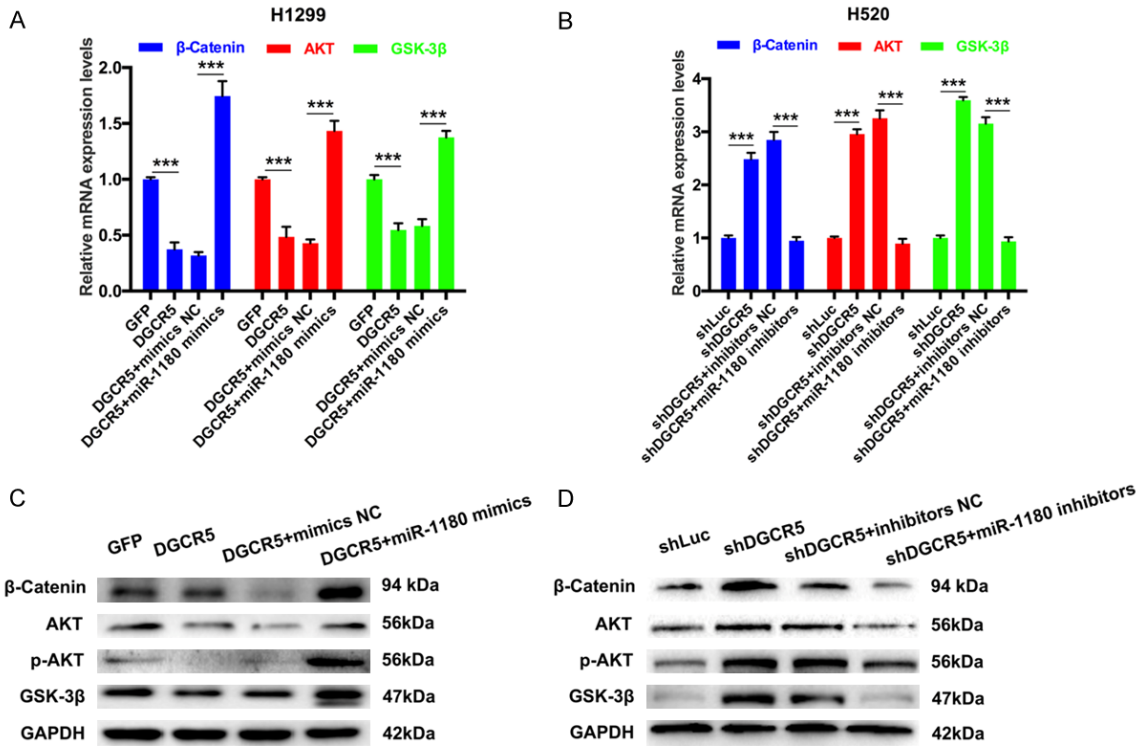

Figure 6. DGCR5 decreased the expression levels of AKT, GSK-3β, and β-catenin through miR-1180. (A) The mRNA expression levels of AKT, GSK-3β, and β-catenin were analyzed by qRT-PCR in H1299 cells transfected with Lenti-GFP, Lenti-DGCR5, Lenti-DGCR5 and mimics NC or Lenti-DGCR5 and miR-1180 mimics (***$P < 0.001$). (B) The expression levels of AKT, GSK-3β, and β-catenin were detected by qRT-PCR in H520 cells transfected with shLuc, shDGCR5, shDGCR5 and inhibitors NC or shDGCR5 and miR-1180 inhibitors (***$P < 0.001$). The protein levels of AKT, p-AKT, GSK-3β, and β-catenin were measured by Western blotting in transfected H1299 (C) and H520 cells (D). GAPDH was used as the loading control.

[28, 29]. In our study, we found that DGCR5 was downregulated in the sera and tissues of LC patients, higher expression of DGCR5 was associated with longer survival in LC patients, and DGCR5 expression was increased in post-operation sera compared with that in pre-operation sera. These data indicated that downregulated DGCR5 in LC patients was associated with poor prognosis. In addition, we found that DGCR5 inhibited the proliferation, migration and invasion of LC cells.

Accumulating evidence has demonstrated that miRNAs have crucial biological functions in tumors, including cell proliferation, inflammation and metastasis by targeting mRNAs [30, 31]. Studies have also confirmed that lncRNAs has the ceRNA activity by acting as miRNA sponges, and they play important roles in human development [32]. In our study, we revealed that miR-1180 was upregulated in the sera and tissues of LC patients, higher expression of miR-1180 was associated with shorter survival in LC patients, and miR-1180 expression was decreased in post-operation sera compared with that in pre-operation sera. Therefore, we suggested that upregulated of miR-1180 was associated with poor prognosis in LC. Furthermore, our results showed that there was a negative correlation between the expression of DGCR5 and miR-1180 in LC tissues and sera. DGCR5 negatively regulated miR-1180 expression. DGCR5 suppressed the proliferation, migration and invasion of LC cells by targeting miR-1180. Another study has demonstrated that miR-1180 enhanced proliferation and apoptotic resistance in hepatocellular carcinoma [33].

Akt, a serine/threonine kinase, is a key regulator downstream of phosphatidylinositol-3 kinase (PI3K) that regulates numerous intracellular signals, affects cell responses to extrinsic stimuli and modulates cell proliferation and survival [34, 35]. Glycogen synthase kinase 3 (GSK-3) is a highly conserved serine/threonine

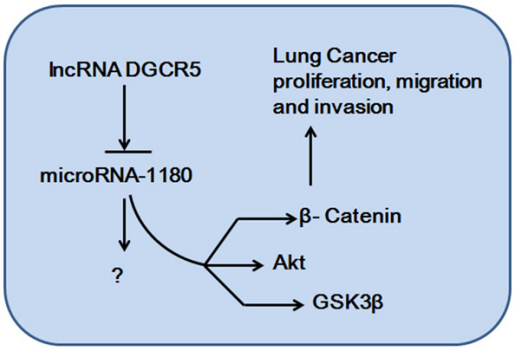

Figure 7. A model of the lncRNA DGCR5/miR-1180 axis in the progression of lung cancer.

protein kinase that can generate two related protein homologs (GSK-3a and GSK-3β) [36]. GSK-3 has important functions in many cellular processes through its activity as a glycogen synthase [37]. This protein kinase is highly active in resting cells but is inhibited in response to cellular signals, including hormone and growth-factor activation of receptor-tyrosine kinases, resulting in the activation of protein kinase B (PKB/Akt) [38]. GSK-3 has important effects on various cellular processes such as gene expression, cell division, glycogen metabolism, survival and apoptosis. GSK-3 has two isoforms: GSK-3α (51 kDa), regulated by phosphorylation at Ser21 and Tyr279, and GSK-3β (47 kDa), regulated by Ser9 and Tyr216 [39]. Akt can phosphorylate GSK-3β at Ser9, and the phosphorylated GSK-3β, due to its decreased GSK-3 activity, is associated with tumorigenesis [40]. GSK-3 is also a major component of the Wnt-signaling pathway [37]. A part of the GSK-3 protein is closely related to the Axin-scaffolding protein, which binds adenomatous polyposis coli (APC) and β-catenin during cellular dormancy [41]. GSK-3-mediated phosphorylation of β-catenin targets leads to ubiquitination and proteosome-mediated degradation [42]. One study has also indicated that β-catenin has a significant effect on Wnt/β-catenin signaling through the canonical pathway [43]. In the absence of the Wnt/β-catenin signaling pathway, β-catenin is bound to axin, adenomatous polyposis coli (APC), and GSK-3β. GSK-3 can phosphorylate β-catenin at Ser37, Ser33, and Thr41, activating ubiquitylation before proteosomal degradation [44, 45]. Signaling through Wnt can downregulate GSK-3β and stabilize β-catenin. Stable β-catenin is translocated from the cytoplasm to nucleus and plays an important role as a transcription cofactor of T cell factor (TCF). Therefore, GSK-3β is correlated with the β-catenin gene regulation mechanism.

In summary, DGCR5 and miR-1180 were differentially expressed and were correlated with prognosis of LC. DGCR5 inhibited proliferation, migration and invasion of LC cells via miR-1180. DGCR5 could directly or indirectly downregulate the expression of AKT, GSK-3β, and β-catenin through miR-1180 (**Figure 7**). Therefore, there is conclusive evidence that the low expression of DGCR5 is involved in the development of LC, and thus, it may serve as a potential therapeutic target for LC.

Disclosure of conflict of interest

None.

Address correspondence to: Hui-Hui Hu, Department of Pulmonary Medicine, Sir Run Run Shaw Hospital of Zhejiang University, No. 3 Qingchun East Road, Hangzhou 310016, Zhejiang Province, China. Tel: 86-0571-86006191; Fax: 86-0571-86006191; E-mail: huhuisection@aliyun.com

References

[1] Oak CH, Wilson D, Lee HJ, Lim HJ and Park EK. Potential molecular approaches for the early diagnosis of lung cancer (review). Mol Med Rep 2012; 6: 931-936.

[2] Yang Q, Xu E, Dai J, Liu B, Han Z, Wu J, Zhang S, Peng B, Zhang Y and Jiang Y. A novel long noncoding RNA AK001796 acts as an oncogene and is involved in cell growth inhibition by resveratrol in lung cancer. Toxicol Appl Pharmacol 2015; 285: 79-88.

[3] Siegel RL, Miller KD and Jemal A. Cancer statistics, 2016. CA Cancer J Clin 2016; 66: 7-30.

[4] Yang YR, Zang SZ, Zhong CL, Li YX, Zhao SS and Feng XJ. Increased expression of the lncRNA PVT1 promotes tumorigenesis in non-small cell lung cancer. Int J Clin Exp Pathol 2014; 7: 6929-6935.

[5] Zeng Z, Bo H, Gong Z, Lian Y, Li X, Li X, Zhang W, Deng H, Zhou M, Peng S, Li G and Xiong W. AFAP1-AS1, a long noncoding RNA upregulated in lung cancer and promotes invasion and metastasis. Tumour Biol 2016; 37: 729-737.

[6] Tanoue LT, Tanner NT, Gould MK and Silvestri GA. Lung cancer screening. Am J Respir Crit Care Med 2015; 191: 19-33.

[7] Wang M, Cao JX, Pan JH, Liu YS, Xu BL, Li D, Zhang XY, Li JL, Liu JL, Wang HB and Wang ZX.

Adoptive immunotherapy of cytokine-induced killer cell therapy in the treatment of non-small cell lung cancer. PLoS One 2014; 9: e112662.
[8] Forde PM and Ettinger DS. Targeted therapy for non-small-cell lung cancer: past, present and future. Expert Rev Anticancer Ther 2013; 13: 745-758.
[9] Rothschild SI. [Advanced and metastatic lung cancer-what is new in the diagnosis and therapy?]. Praxis (Bern 1994) 2015; 104: 745-750.
[10] Muller M, Schouten RD, De Gooijer CJ and Baas P. Pembrolizumab for the treatment of non-small cell lung cancer. Expert Rev Anticancer Ther 2017; 17: 399-409.
[11] Leventakos K and Mansfield AS. Advances in the treatment of non-small cell lung cancer: focus on nivolumab, pembrolizumab, and atezolizumab. BioDrugs 2016; 30: 397-405.
[12] Dempke WC and Fenchel K. Pembrolizumab as first-line treatment for non-small cell lung cancer-a game changer? Transl Lung Cancer Res 2016; 5: 538-542.
[13] Costa FF. Non-coding RNAs: Meet thy masters. Bioessays 2010; 32: 599-608.
[14] Okamura K, Chung WJ, Ruby JG, Guo H, Bartel DP and Lai EC. The Drosophila hairpin RNA pathway generates endogenous short interfering RNAs. Nature 2008; 453: 803-806.
[15] Kawaji H and Hayashizaki Y. Exploration of small RNAs. PLoS Genet 2008; 4: e22.
[16] Yao Y and Sun Q. Exploration of small non coding RNAs in wheat (Triticum aestivum L). Plant Mol Biol 2012; 80: 67-73.
[17] Shukla GC, Singh J and Barik S. MicroRNAs: processing, maturation, target recognition and regulatory functions. Mol Cell Pharmacol 2011; 3: 83-92.
[18] Fabian MR, Sonenberg N and Filipowicz W. Regulation of mRNA translation and stability by microRNAs. Annu Rev Biochem 2010; 79: 351-379.
[19] Xia JT, Chen LZ, Jian WH, Wang KB, Yang YZ, He WL, He YL, Chen D and Li W. MicroRNA-362 induces cell proliferation and apoptosis resistance in gastric cancer by activation of NF-kappaB signaling. J Transl Med 2014; 12: 33.
[20] Yang S, Li Y, Gao J, Zhang T, Li S, Luo A, Chen H, Ding F, Wang X and Liu Z. MicroRNA-34 suppresses breast cancer invasion and metastasis by directly targeting Fra-1. Oncogene 2013; 32: 4294-4303.
[21] Wan L, Zhang L, Fan K, Cheng ZX, Sun QC and Wang JJ. Knockdown of long noncoding RNA PCAT6 inhibits proliferation and invasion in lung cancer cells. Oncol Res 2016; 24: 161-170.
[22] Nie W, Ge HJ, Yang XQ, Sun X, Huang H, Tao X, Chen WS and Li B. LncRNA-UCA1 exerts oncogenic functions in non-small cell lung cancer by targeting miR-193a-3p. Cancer Lett 2016; 371: 99-106.
[23] Huang R, Wang X, Zhang W, Zhangyuan G, Jin K, Yu W, Xie Y, Xu X, Wang H and Sun B. Down-regulation of LncRNA DGCR5 correlates with poor prognosis in hepatocellular carcinoma. Cell Physiol Biochem 2016; 40: 707-715.
[24] Farazi TA, Hoell JI, Morozov P and Tuschl T. MicroRNAs in human cancer. In: editors. MicroRNA cancer regulation. Springer; 2013. pp. 1-20.
[25] Djuranovic S, Nahvi A and Green R. A parsimonious model for gene regulation by miRNAs. Science 2011; 331: 550-553.
[26] Kasinski AL and Slack FJ. MicroRNAs en route to the clinic: progress in validating and targeting microRNAs for cancer therapy. Nat Rev Cancer 2011; 11: 849-864.
[27] Di Leva G and Croce CM. The role of microRNAs in the tumorigenesis of ovarian cancer. Front Oncol 2013; 3: 153.
[28] Whitehead J, Pandey GK and Kanduri C. Regulation of the mammalian epigenome by long noncoding RNAs. Biochim Biophys Acta 2009; 1790: 936-947.
[29] Li L, Feng T, Lian Y, Zhang G, Garen A and Song X. Role of human noncoding RNAs in the control of tumorigenesis. Proc Natl Acad Sci U S A 2009; 106: 12956-12961.
[30] Wang J, Paris PL, Chen J, Ngo V, Yao H, Frazier ML, Killary AM, Liu CG, Liang H and Mathy C. Next generation sequencing of pancreatic cyst fluid microRNAs from low grade-benign and high grade-invasive lesions. Cancer Lett 2015; 356: 404-409.
[31] Stahlhut C and Slack FJ. MicroRNAs and the cancer phenotype: profiling, signatures and clinical implications. Genome Med 2013; 5: 111.
[32] Sanchez-Mejias A and Tay Y. Competing endogenous RNA networks: tying the essential knots for cancer biology and therapeutics. J Hematol Oncol 2015; 8: 220-229.
[33] Tan G, Wu L, Tan J, Zhang B, Tai WC, Xiong S, Chen W, Yang J and Li H. MiR-1180 promotes apoptotic resistance to human hepatocellular carcinoma via activation of NF-kappaB signaling pathway. Sci Rep 2016; 6: 22328.
[34] Sukawa Y, Yamamoto H, Nosho K, Kunimoto H, Suzuki H, Adachi Y, Nakazawa M, Nobuoka T, Kawayama M, Mikami M, Matsuno T, Hasegawa T, Hirata K, Imai K and Shinomura Y. Alterations in the human epidermal growth factor receptor 2-phosphatidylinositol 3-kinase-v-Akt pathway in gastric cancer. World J Gastroenterol 2012; 18: 6577-6586.
[35] Wang YQ, Zhang JR, Li SD, He YY, Yang YX, Liu XL and Wan XP. Aberrant methylation of breast and ovarian cancer susceptibility gene 1 in

chemosensitive human ovarian cancer cells does not involve the phosphatidylinositol 3'-kinase-Akt pathway. Cancer Sci 2010; 101: 1618-1623.
[36] Frame S and Cohen P. GSK3 takes centre stage more than 20 years after its discovery. Biochem J 2001; 359: 1-16.
[37] Doble BW and Woodgett JR. GSK-3: tricks of the trade for a multi-tasking kinase. J Cell Sci 2003; 116: 1175-1186.
[38] Liu CW, Yang F, Cheng SZ, Liu Y, Wan LH and Cong HL. Rosuvastatin postconditioning protects isolated hearts against ischemia-reperfusion injury: the role of radical oxygen species, PI3K-Akt-GSK-3 pathway, and mitochondrial permeability transition pore. Cardiovasc Ther 2017; 35: 3-9.
[39] Forde JE and Dale TC. Glycogen synthase kinase 3: a key regulator of cellular fate. Cell Mol Life Sci 2007; 64: 1930-1944.
[40] Gartner A, Huang X and Hall A. Neuronal polarity is regulated by glycogen synthase kinase-3 (GSK-3beta) independently of Akt/PKB serine phosphorylation. J Cell Sci 2006; 119: 3927-3934.
[41] Alexandrova EM and Sokol SY. Xenopus Axin-related protein: a link between its centrosomal localization and function in the Wnt/beta-catenin pathway. Dev Dyn 2010; 239: 261-270.
[42] Amit S, Hatzubai A, Birman Y, Andersen JS, Ben-Shushan E, Mann M, Ben-Neriah Y and Alkalay I. Axin-mediated CKI phosphorylation of beta-catenin at Ser 45: a molecular switch for the Wnt pathway. Genes Dev 2002; 16: 1066-1076.
[43] Nelson WJ and Nusse R. Convergence of Wnt, beta-catenin, and cadherin pathways. Science 2004; 303: 1483-1487.
[44] Kipreos ET, Lander LE, Wing JP, He WW and Hedgecock EM. cul-1 is required for cell cycle exit in C. elegans and identifies a novel gene family. Cell 1996; 85: 829-839.
[45] Fuchs SY, Chen A, Xiong Y, Pan ZQ and Ronai Z. HOS, a human homolog of Slimb, forms an SCF complex with Skp1 and Cullin1 and targets the phosphorylation-dependent degradation of IkappaB and beta-catenin. Oncogene 1999; 18: 2039-2046.

Supplementary Table 1. Part I RegRNA predited DGCR5 regulated miRNAs

No.	miRNA ID	Location	Len	Minimum free energy
1	hsa-let-7b	494~519	26	-27.7
2	hsa-miR-1180	59~82	24	-26.4
3	hsa-miR-1181	30~52	23	-28.8
4	hsa-miR-1183	432~458	27	-26.4
5	hsa-miR-1225-3p	2050~2072	23	-29.2
6	hsa-miR-1233	2437~2455	19	-26.8
		2437~2455	19	-26.8
7	hsa-miR-1254	3090~3121	32	-26.7
8	hsa-miR-1296	2435~2457	23	-26.3
		2511~2537	27	-27.2
9	hsa-miR-1469	2909~2929	21	-30.6
10	hsa-miR-1470	3009~3029	21	-30.3
11	hsa-miR-1538	2905~2932	28	-28.9
12	hsa-miR-185*	2230~2252	23	-26.5
13	hsa-miR-1976	1885~1905	21	-28.1
14	hsa-miR-2277-3p	2439~2459	21	-27.2
15	hsa-miR-2861	985~1003	19	-29.2
16	hsa-miR-298	824~851	28	-26.3
17	hsa-miR-3130-5p	69~89	21	-33.8
		69~89	21	-33.8
18	hsa-miR-3132	1399~1422	24	-27.7
		3044~3066	23	-26.9
19	hsa-miR-3154	1286~1307	22	-26.2
20	hsa-miR-3177	2977~2997	21	-28
21	hsa-miR-3180-3p	71~97	27	-30.3
		71~97	27	-30.3
		71~97	27	-30.3
22	hsa-miR-3180	74~97	24	-28.2
		74~97	24	-28.2
23	hsa-miR-3181	46~69	24	-28.9
24	hsa-miR-3189	339~365	27	-26.6
25	hsa-miR-3194	2054~2075	22	-27.3
26	hsa-miR-3196	107~126	20	-26.2
27	hsa-miR-324-5p	2051~2073	23	-26.6
28	hsa-miR-339-3p	3154~3174	21	-27.4
29	hsa-miR-3605-3p	2879~2905	27	-27.3
30	hsa-miR-3619	2832~2853	22	-30.2
31	hsa-miR-3621	104~123	20	-29.3
32	hsa-miR-3907	321~341	21	-27
33	hsa-miR-3937	458~480	23	-29.9
34	hsa-miR-3943	2042~2071	30	-33.9
35	hsa-miR-3944	38~69	32	-41.6
36	hsa-miR-4254	2667~2687	21	-27.5
37	hsa-miR-4259	475~498	24	-29.1
38	hsa-miR-4292	54~71	18	-28.2

39	hsa-miR-4298	2244~2266	23	-27
40	hsa-miR-4322	987~1006	20	-26.7
41	hsa-miR-486-5p	2863~2884	22	-28.8
42	hsa-miR-508-5p	142~163	22	-28.1
43	hsa-miR-612	3095~3119	25	-29.1
		850~881	32	-26.93
44	hsa-miR-637	1932~1955	24	-27.1
		2966~2989	24	-31.6
45	hsa-miR-638	80~115	36	-35.8
46	hsa-miR-657	1850~1871	22	-27.2
47	hsa-miR-661	979~1001	23	-26.8
48	hsa-miR-663	107~129	23	-37.7
		455~478	24	-32.3
49	hsa-miR-665	820~840	21	-26.6
		2527~2545	19	-26.3
50	hsa-miR-762	44~67	24	-31.2
		304~334	31	-26.91
51	hsa-miR-939	456~476	21	-30.2
		3090~3114	25	-29.4
52	hsa-miR-940	3016~3048	33	-28.1